Molecular Microbiology (2017) 103(1), 26–38 ■
doi:10.1111/mmi.13575
First published online 25 November 2016

EspC forms a filamentous structure in the cell envelope of *Mycobacterium tuberculosis* and impacts ESX-1 secretion

Ye Lou,[1] Jan Rybniker,[1,2†] Claudia Sala[1] and Stewart T. Cole[1]*
[1]*Global Health Institute, Ecole Polytechnique Fédérale de Lausanne (EPFL), Lausanne, CH-1015, Switzerland.*
[2]*1st Department of Internal Medicine, University of Cologne, Cologne, D-50937, Germany.*

Summary

Pathogenicity of *Mycobacterium tuberculosis* (*M. tb*) is mediated by the ESX-1 secretion system, which exports EsxA and EsxB, the major virulence factors that are co-secreted with EspA and EspC. Functional information about ESX-1 components is scarce. Here, it was shown that EspC associates with EspA in the cytoplasm and membrane, then polymerizes during secretion from *M. tb*. EspC was localized by immuno-gold electron microscopy in whole cells or cryosections as a surface-exposed filamentous structure that seems to span the cell envelope. Consistent with these findings, purified EspC homodimerizes via disulphide bond formation, multimerizes and self-assembles into long filaments *in vitro*. The C-terminal domain is required for multimerization as truncation and selected point mutations therein impact EspC filament formation, thus reducing secretion of EsxA and causing attenuation of *M. tb*. The data are consistent with EspC serving either as a modulator of ESX-1 function or as a component of the secretion apparatus.

Introduction

Mycobacterium tuberculosis (*M. tb*) is a leading cause of human morbidity and mortality despite the availability of effective treatment (Zumla *et al.*, 2015). Of the five type VII secretion systems (T7SS) present in *M. tb* (ESX-1–5) the ESX-1 secretion system is employed for virulence factor export and host-pathogen interaction (Stanley *et al.*, 2003; Simeone *et al.*, 2009). The ESX-1 core components (Ecc proteins) and most of the known substrates (Esx or Esp proteins) are encoded by the *esx-1* locus, which spans 20 genes. Deletion of *esx-1* causes severe attenuation of virulence in cellular and animal models of infection (Pym *et al.*, 2002; Guinn *et al.*, 2004; Brodin *et al.*, 2006; Stoop *et al.*, 2012). Of the known ESX-1 substrates, two small proteins, EsxA and EsxB, are major virulence factors and immunodominant T-cell antigens (Wards *et al.*, 2000; Renshaw *et al.*, 2002; Simeone *et al.*, 2009).

EsxA and EsxB form a heterodimer *in vitro* and dissociate at low pH, which might facilitate the interaction of EsxA with host cell membranes upon release from its chaperone, EsxB, in the acidic environment of the macrophage phagosome. EsxA lyses membranes (Hsu *et al.*, 2003) thereby enabling phagosomal escape and intra- and intercellular spread of the bacteria (Renshaw *et al.*, 2002; De Jonge *et al.*, 2007; Smith *et al.*, 2008; Simeone *et al.*, 2009; Vandal *et al.*, 2009; De Leon *et al.*, 2012). The distal *espACD* operon, which is restricted to pathogenic mycobacteria, including *Mycobacterium leprae* with its downsized genome (Cole *et al.*, 2001), is also necessary for ESX-1 secretion and function. Figure 1a displays the organization of the unlinked *espACD* and *esx-1* gene clusters in three pathogenic mycobacteria that secrete EsxA/B during infection. The EspA and EspC proteins are both ESX-1 substrates and required for EsxA/EsxB secretion (Fortune *et al.*, 2005; Champion *et al.*, 2009).

The mechanism of ESX-1 secretion and the structure and composition of the secretory apparatus are still unclear. Most of the identified T7SS substrates carry a YxxxD motif, located approximately 80–90 amino acid residues from the N-terminus, as the general secretion signal (Daleke *et al.*, 2012). In the now well-accepted model, they are recognized in the cytosol via this signal sequence and targeted to the inner-membrane where a membrane-associated complex comprising the ATPase EccC, the putative channel protein, EccD, as well as EccB and EccE, is involved in translocation of substrates across the cytoplasmic membrane (Champion *et al.*, 2006; Bitter *et al.*, 2009; Champion *et al.*, 2009; Houben *et al.*, 2012). However, it is not known, nor even

Accepted 7 November, 2016. *For correspondence. E-mail stewart.cole@epfl.ch; Tel. +4121693 18 51; Fax +41 21 693 17 90. †Present address: German Center for Infection Research (DZIF), Partner Site Bonn-Cologne, Cologne, Germany.

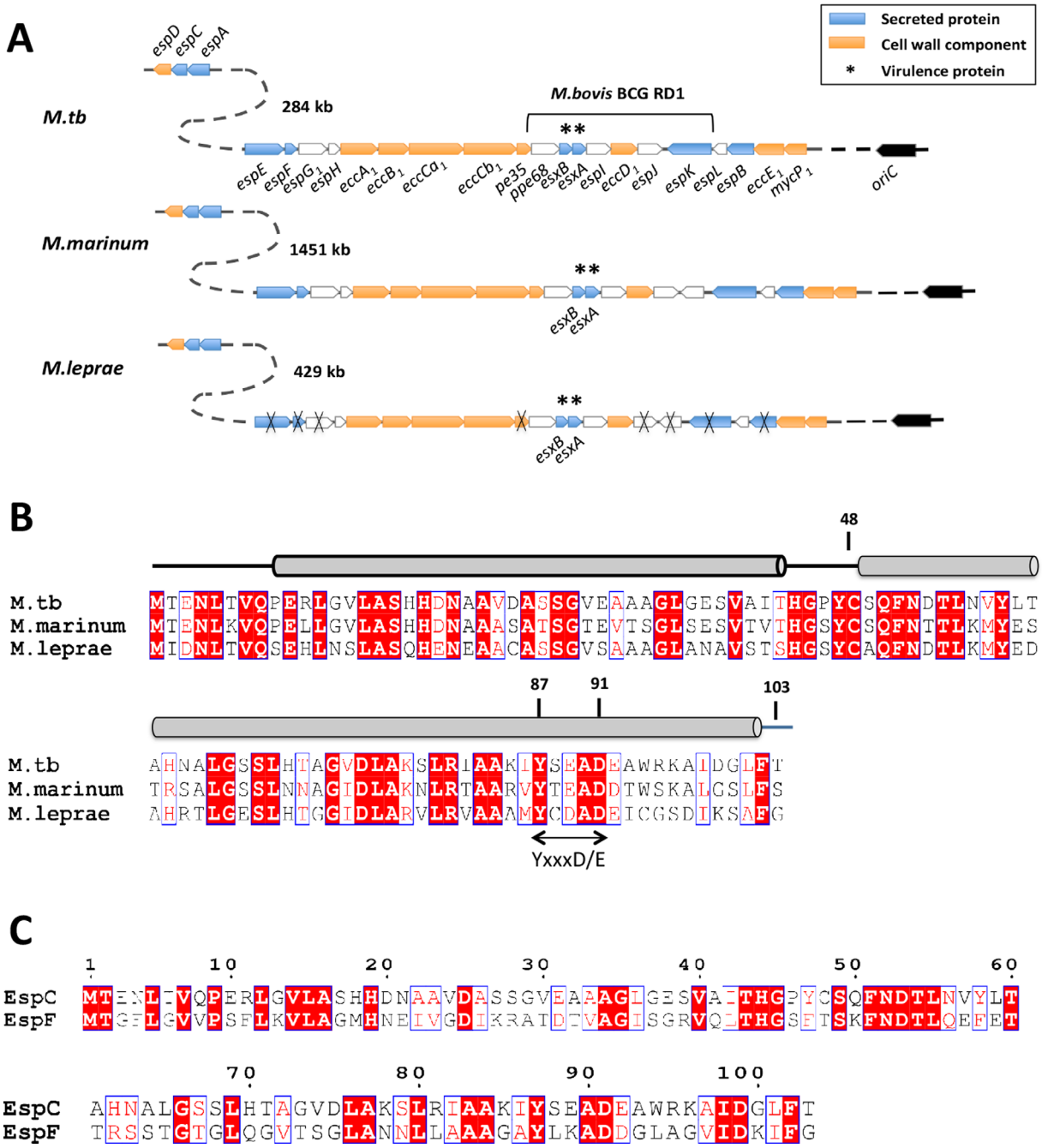

Fig. 1. Genetic organization of *espACD* and *esx-1* loci and EspC structural elements in three mycobacterial pathogens.
A. Comparison of genetic loci important for ESX-1 function in pathogenic mycobacteria. Genes are color-coded according to the localization of their proteins—see key. White denotes no information available, crosses denote pseudogenes.
B. Primary and secondary structure alignments of EspC proteins derived from the same pathogens showing location of conserved Cys-48 and the YxxxD/E motif. Secondary structure analysis by PSI-PRED suggests that EspC is composed of two alpha helices (grey cylinders) connected by a loop. Identical and similar residues are shown in red and white boxes respectively.
C. Primary structure alignment of EspC and EspF from *M. tb*.

predictable bioinformatically, which proteins form the channel through the multilayered mycobacterial cell wall (termed mycomembrane or outer-membrane). One of the obstacles in addressing this question is the complexity of the mycomembrane (Brennan and Nikaido, 1995) where the ESX-1 apparatus is partly embedded. In contrast to the Gram-negative bacteria (e.g. *Escherichia coli* containing more than 60 outer membrane proteins), only two

porins, MctB and OmpATb, have been found in *M. tb* thus far (Van der Woude *et al.*, 2013). Moreover, genome comparisons failed to find a candidate for an outer membrane pore protein that is related to ESX-1 secretion (Mah *et al.*, 2010; Niederweis *et al.*, 2010). Adding to the challenge, the cell surface of *M. tb* is covered by a thick capsular layer. Several ESX-1-associated proteins were identified in capsule extracts of *Mycobacterium marinum*, but the ESX-1 apparatus has not been directly visualized (Sani *et al.*, 2010).

Here, we investigated the role of EspC in the ESX-1 secretion system. EspC is a small protein with a YxxxD motif, which is also a highly specific T-cell antigen (Millington *et al.*, 2011). Given the co-dependent manner of secretion of EsxA/EsxB, and EspA/EspC, it is likely that these proteins interact or form a complex during translocation (Champion *et al.*, 2009; Das *et al.*, 2011). Our functional investigation of EspC provides new insight into the ESX-1 secretion mechanism. We reveal that EspC interacts initially with EspA in the cytoplasm and then in the cell membrane before polymerizing during export into a filament that seemingly spans the capsule of *M. tb* and is surface-exposed.

Results

The EspC protein of pathogenic mycobacteria

Most mycobacteria contain an *esx-1* locus located near *oriC*, the chromosomal origin of replication, but only the pathogens possess the distally located *espACD* gene cluster (Fig. 1A). An alignment of the EspC proteins revealed strict conservation of 45 of the 103 amino acid residues. Prominent among these were the YxxxD/E motif (Y87-D91) and a single cysteine residue (Cys-48). Secondary structure predictions indicate that EspC, like the cytolytic EsxA and other Esx-family proteins, comprises two alpha helices connected by a short loop (Fig. 1B).

A second paralogous copy of this cluster, comprising *espEFG$_1$H*, occurs at the 5′-end of the *esx-1* locus in *M. tb*, and *M. marinum*. In *M. leprae*, the *espEFG$_1$* genes have undergone pseudogenization so cannot contribute to EsxA/B secretion. In *M. tb*, EspF is also 103 amino acids long, shares 37 identical residues, including the YxxxD motif, with EspC and is also predicted to contain two alpha helices. Both EspC and EspF have been detected by proteomics but our quantification of gene expression analysis by RNA-Seq revealed the EspC transcript to be approximately twofold more abundant (see Supporting Information).

EspC polymerizes upon secretion from M. tb

As all our attempts to raise specific EspC antibodies were unsuccessful, we produced a haemagglutinin (HA) epitope-tagged form by inserting the HA coding sequence after the start codon of *espC*. To ensure that the resultant HA-tagged EspC, which was readily detected by the cognate murine monoclonal antibody, retained full activity a complementation experiment was undertaken with an *espC* transposon insertion mutant (*espC*::Tn) of *M. tb*. We introduced the pMD31-*espAC$_{HA}$D* construct into the *espC*::Tn mutant (Fig. 2A) in order to test for ESX-1 function. Use of the entire *espACD* cluster was required since the three genes are co-transcribed (Daugelat *et al.*, 2003); transformants bearing the empty vector pMD31 failed to produce EspC or to secrete EsxA. By contrast, the ESX-1 secretion system of the *espC*::Tn + *espAC$_{HA}$D* strain was fully functional since EsxA was detected in the culture filtrate in normal amounts (Fig. 2A). Thus, HA-tagging did not noticeably affect function and allowed for further characterization of EspC.

EspC in the cell membrane and cytosol that were obtained from cell lysates by ultracentrifugation, as well as in the culture filtrate, were analyzed by SDS-PAGE and immunoblotting. Whereas EspC was monomeric in the cytosol of *M. tb*, it appeared as multiple SDS-stable, high molecular weight species in the envelope and culture filtrate, thereby implying that EspC polymerization occurs during secretion. On the other hand, most of the EsxA was secreted into the culture medium and was undetectable in the cell membrane fraction (Fig. 2B). Since ESX-1 substrates have been detected in the capsular layer of *M. marinum* (Sani *et al.*, 2010), we also examined this cellular compartment for EspC. The capsule of mycobacteria can be removed by extraction with a detergent such as Tween-80 that is usually added to cultures to prevent clumping (Sani *et al.*, 2010). Strain *espC*::Tn + *espAC$_{HA}$D* was grown in Sauton's medium, with or without Tween-80, to mid-log phase. After extraction with the mild detergent Genapol X-080, capsular proteins were TCA-precipitated and analyzed by immunoblotting. While EsxA was below the limit of detection, HA-tagged EspC was clearly detectable in the *M. tb* capsule extract from *espC*::Tn + *espAC$_{HA}$D* cells grown without Tween-80 but was completely absent when these cells had been grown with Tween-80 or when the *espC*::Tn + pMD31 mutant was used (Fig. 2C and data not shown). Capsular EspC was still present in an SDS-resistant multimeric form despite the Genapol extraction and TCA-precipitation. By comparing the respective band intensities in culture filtrates, EspC was much more abundant in the cell envelope, where EsxA was undetectable. These results indicate that EspC is distinct from EsxA in function, despite the structural similarities.

Given that a cysteine is present in EspC and potentially involved in intermolecular interaction, we assessed

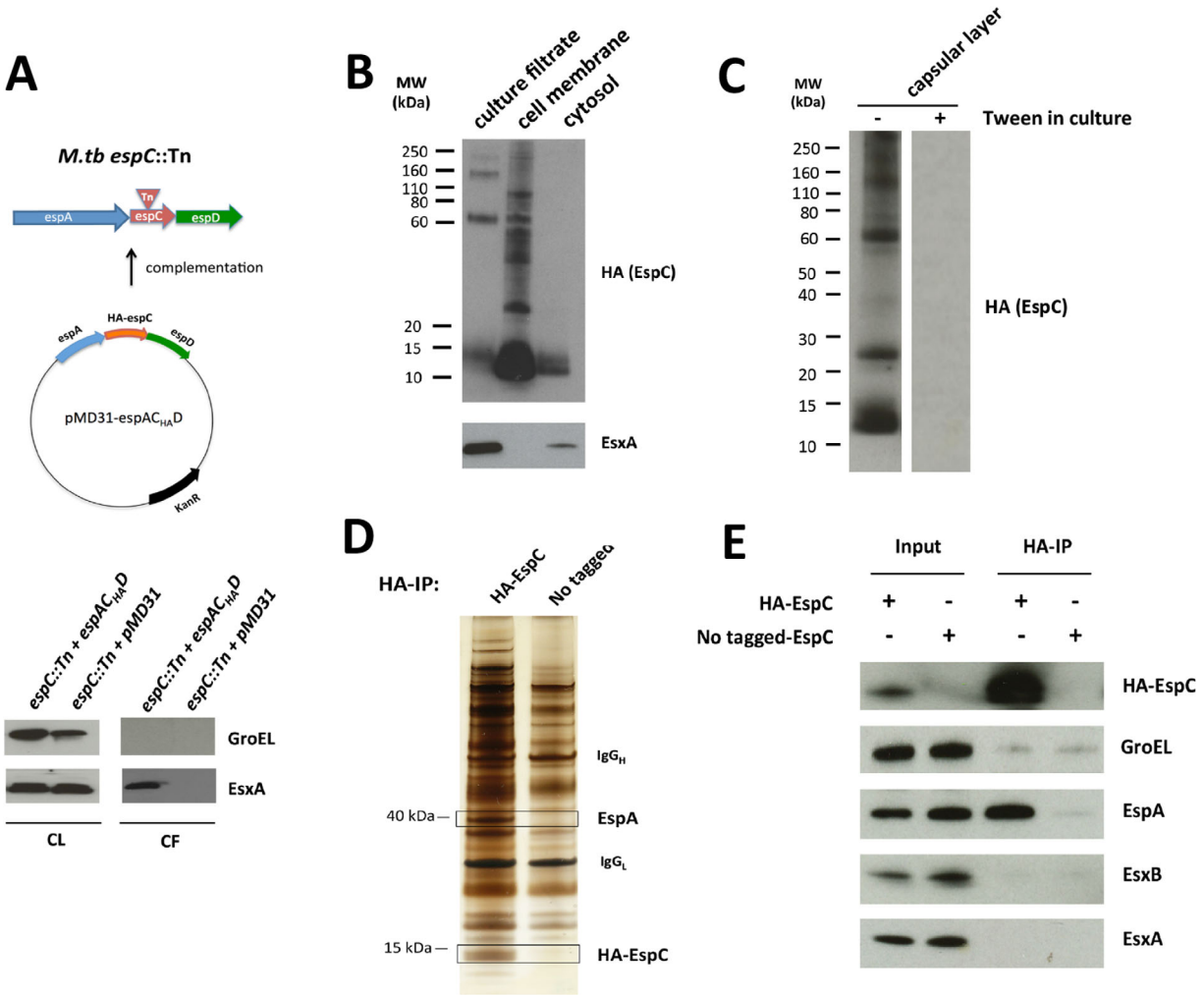

Fig. 2. EspC binds to EspA inside cells and polymerizes upon secretion from *M. tb*.
A. Scheme showing complementation of the *M. tb espC*::Tn mutant with pMD31-*espAC$_{HA}$D*, encoding N-terminally HA-tagged EspC, or the empty vector. EsxA secretion was restored by complementation.
B. Culture filtrate proteins (15 μg), cell membrane proteins (5 μg) or cytosolic proteins (5 μg) were boiled in SDS buffer and electrophoresed on an SDS-PAGE gel. EspC was detected using an anti-HA antibody conjugated with HRP. In the cytosol, EspC was monomeric. In the cell membrane and culture filtrate, EspC formed SDS-resistant polymer. Most of the EsxA was secreted into culture medium.
C. Bacteria were cultured in Sauton's medium with or without Tween-80 and extracted with Genapol X-080 to enrich capsular layer proteins. TCA-precipitated proteins (10 μg) were separated by SDS-PAGE then immunoblotted. EspC was detectable in the capsular layer extract, whereas EsxA was not.
D. Pull-down experiment in which beads coated with monoclonal antibodies targeting the HA-tag were incubated with crude cell lysates containing either native EspC or HA-tagged EspC. Note the presence of a 40 kDa protein, identified by LC-MS/MS as EspA (Spectrum count: 18; Sequence coverage: 37%), only when HA-tagged EspC was used.
E. Immunoblot demonstrating interaction between EspA-EspC in cell lysates. Antibodies used are indicated at right.

the effect of DTT on the multimeric state of EspC produced in *M. tb*. Notably, the polymeric forms in the culture filtrate were reduced by DTT treatment to lower molecular weight forms, indicating the role of disulphide bond formation in polymer assembly (Supporting Information Fig. S1). Stabilization of EspC by Cys-48 is supported by our finding that its replacement by serine in strain *espC*::Tn + *espAC^{C48S}D* decreased the amount of EspC to below the level of detection thereby ablating EsxA secretion (Supporting Information Fig. S2).

EspC interacts with EspA in the cytoplasm and cell membrane

As EspC forms an SDS-resistant polymer during secretion, a molecular chaperone should be required for EspC to keep its monomeric form in the cell. This role may be played by the AAA+ ATPase EccA1, which uses its TPR domain to bind the C-terminus of EspC (Champion *et al.*, 2009). However, YxxxD proteins are expected to interact with a WxG100 partner protein and in the case of EspC the likely candidate is EspA (Das *et al.*, 2011;

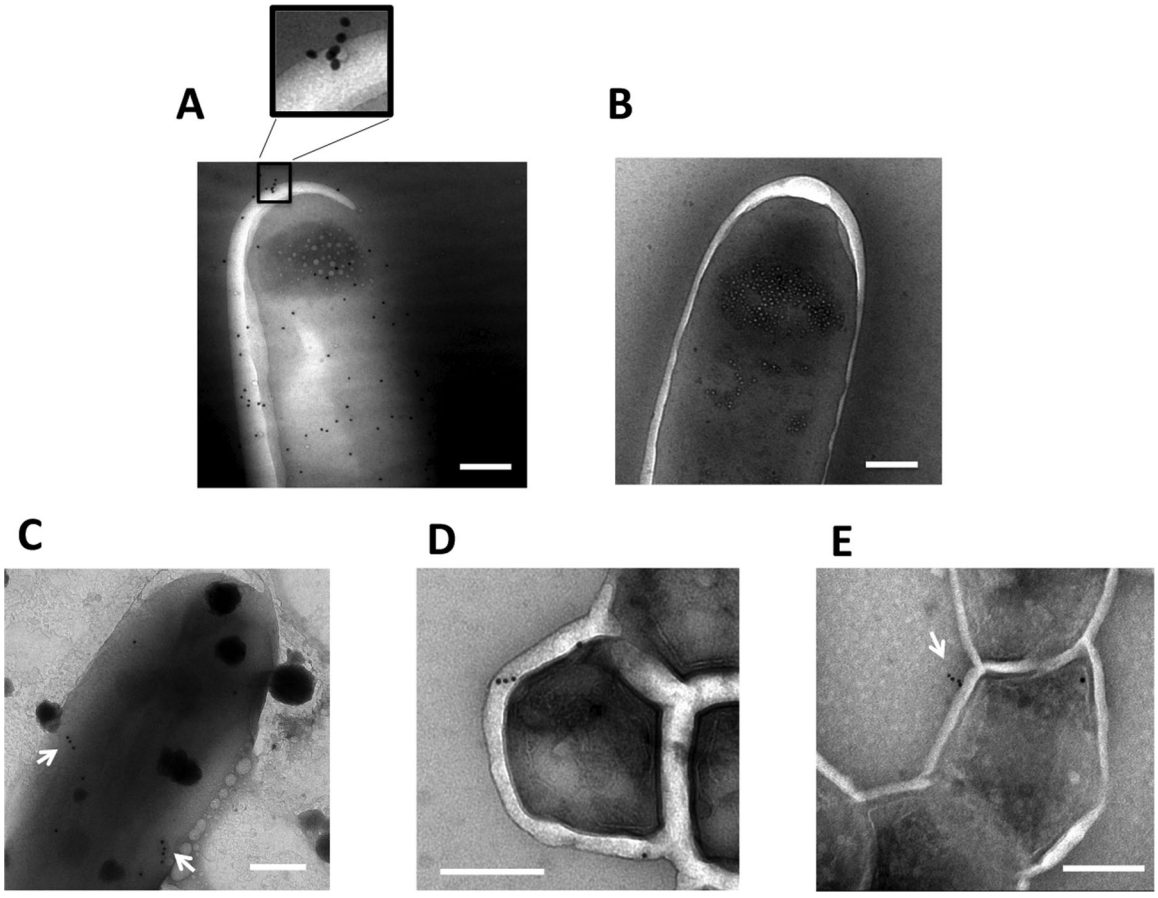

Fig. 3. EspC exists as surface-exposed filaments in *M. tb*.
A. Immunogold-EM analysis of whole cell mounts of *M. tb* reveals EspC on cell surface.
B. Strain *espC*::Tn+pMD31 used as a negative control.
C. Whole cells grown without Tween-80 after extraction with 0.025% Genapol X-080.
D, E. Cryo-sections of cells grown without Tween-80. Surface-exposed EspC was stained with anti-HA antibody and 10 nm gold-conjugated anti-mouse IgG. Scale bar: 200 nm. Arrows indicate EspC filaments.

Solomonson *et al.*, 2015). To identify potential partners, we exploited the ability of beads coated with HA-antibodies to capture the HA-tagged form of EspC present in total cell lysates. On analysis of the silver-stained proteins bound to such beads, a single 40 kDa species was present when HA-tagged EspC was used but not when native EspC was employed (Fig. 2D; Supporting Information Fig. S3A). This species was identified by LC-MS/MS analysis, after trypsin digestion, as EspA (Spectrum count: 18; Sequence coverage: 37%). These results were confirmed by immunoblotting using HA-antibodies and EspA-specific antibodies (Fig. 2E). This demonstrated a specific interaction between EspA and EspC in cell lysates but not between EspC and EsxA or EsxB. To establish whether EspA interacts with EspC in the cytosol, cell membrane fraction or both, the immunoprecipitation experiment was repeated with subcellular fractions of the cell lysate. EspA co-precipitated with HA-tagged EspC from both the cytosolic and membrane fractions and appeared to be more abundant in the latter (Supporting Information Fig. S3B). EspA also contains a single cysteine residue, Cys-138, that could potentially form a disulphide bond. However, replacement of Cys-138 by alanine did not affect its interaction with His-tagged EspC in *M. tb* (Supporting Information Fig. S4).

EspC forms bacterial surface-exposed filaments

We have shown that polymeric EspC is abundant in the capsular layer. To verify this observation, immunogold-labelling was then employed to visualize EspC on the surface of intact *M. tb* cells by transmission electron microscopy (TEM). When bacteria were grown in Sauton's medium lacking Tween-80, the capsular layers were clearly seen as a transparent zone outside the cell (Fig. 3A, B). EspC labelling was randomly distributed along the surface of all of the *espC*::Tn + $espAC_{HA}D$ cells examined (Fig. 3A), whereas the *espC*::Tn + pMD31

mutant showed no labelling (Fig. 3B). Independent confirmation of this finding was obtained by immunofluorescence microscopy using secondary antibodies labelled with the fluorescent dye Alexa-488 where again all cells displayed fluorescence (Supporting Information Fig. S5).

EspC filaments buried in the polysaccharide-rich capsular layer are likely to be inaccessible to the antibody-conjugated gold probes. As shown in the inset to Fig. 3A, only when extending beyond the capsular layer was EspC detected in clusters or as a filament. Such filaments were found in about 50% of the cells inspected. Therefore, in the next experiments, we made the capsule more permeable for immuno-labelling. After treatment with diluted Genapol X-080, the capsule was partially removed from intact cells, while the association of EspC with the cell envelope was not seriously disrupted as evidenced by a filamentous arrangement of EspC, labelled with gold beads, on the cell surface (Fig. 3C). The use of cryo-sections also enhances the accessibility of antibodies to the subunits of EspC filaments. Thin-sections of cells again displayed EspC filaments within (Fig. 3D) and beyond (Fig. 3E) the electron transparent zone of the cell envelope, and exposed on the surface of *M. tb* and these were detected in about 25% of the sections examined.

Purification, oligomerization and filament formation of recombinant EspC

To further investigate the multimeric state of EspC *in vitro*, we overexpressed and purified an N-terminally His-tagged form from *E. coli* (Supporting Information Fig. S6). However, since the solubility was low we adopted a mycobacterial expression system, based on the *M. smegmatis groEL1ΔC* strain (Daugelat *et al*., 2003; Noens *et al*., 2011), thereby improving solubility and enabling purification to homogeneity.

As expected, EspC was predominantly expressed as a polymer with an estimated molecular weight of >100 kDa according to size exclusion chromatography (Fig. 4A). Circular dichroism (CD) spectroscopy indicated that the polymer was mainly composed of α-helices (Fig. 4B). Urea-denatured EspC could refold and self-associate into a polymer of similar size to the native state (Fig. 4A). As shown previously, EspC has a single cysteine residue, Cys-48, that partially contributes to polymer formation in *M. tb*. The dimer of purified EspC, visible by SDS-PAGE, was converted to a monomer when treated with the reducing agents β-mercaptoethanol (BME) or dithiothreitol (DTT), also implying the presence of intermolecular disulphide bonds in the EspC polymer (Fig. 4C).

Lowering the NaCl concentration caused purified EspC to further self-assemble into filaments. Electron micrographs of negatively stained EspC revealed that the filaments elongated over time (Fig. 4D). After 5 days, EspC existed predominantly as long filaments of approximately 10–15 nm diameter. Formation of a filamentous structure from affinity-purified EspC is consistent with what was observed in *M. tb*.

EspC is not membranolytic

Secreted EsxA damages the phagosomal membrane thereby enabling *M. tb* to escape from the phagosome (De Jonge *et al*., 2007; Simeone *et al*., 2009; De Leon *et al*., 2012). To establish whether EspC, which resembles EsxA in length and predicted structure, can lyse membranes, we performed a macrophage cytotoxicity assay in which the intracellular potassium level was used to monitor the viability of RAW 264.7 cells after exposure to purified EspC for 2 h. Unlike EsxA, which caused massive potassium efflux, EspC had no detectable cytolytic activity (Supporting Information Fig. S7).

The C-terminus of EspC mediates polymer formation, stability and mycobacterial virulence

Since the EspC polymer exported from *M. tb* was not fully disrupted by DTT (Supporting Information Fig. S1), and purified $EspC^{C48S}$ still polymerizes (Supporting Information Fig. S8), we reasoned that additional features might be essential for EspC assembly. On the basis of similarity in sequence and structure to the YxxxD/E region of EspB, Solomonson *et al*. have proposed that the C-terminus of EspC, and its paralogs, may serve as an 'export arm' (Solomonson *et al*., 2015). The 'export arm' region harbouring a secretion signal YxxxD motif, as well as a C-terminal tail which was identified to be essential for ESX substrate secretion (Sysoeva *et al*., 2014) (Fig. 5A).

Thus, a C-terminally truncated form lacking the last six amino acid residues, $EspC^{C\Delta6}$, was constructed. In contrast to $EspC^{wt}$, the $EspC^{C\Delta6}$ protein was predominantly monomeric (Fig. 5B). To further understand the importance of the C-terminal tail, the HA-tagged $EspC^{C\Delta6}$ was introduced into *M. tb* strain *espC*::Tn, then assessed for its stability, export and impact on EsxA secretion. We found that the truncation rendered EspC unstable in cells (Fig. 5C), thereby abolishing EsxA secretion (Fig. 5D) and severely attenuating bacterial virulence (Fig. 5E). We next investigated individual residues within this region. This revealed that the $EspC^{I98A}$ variant, exhibiting a profile containing a mixture of

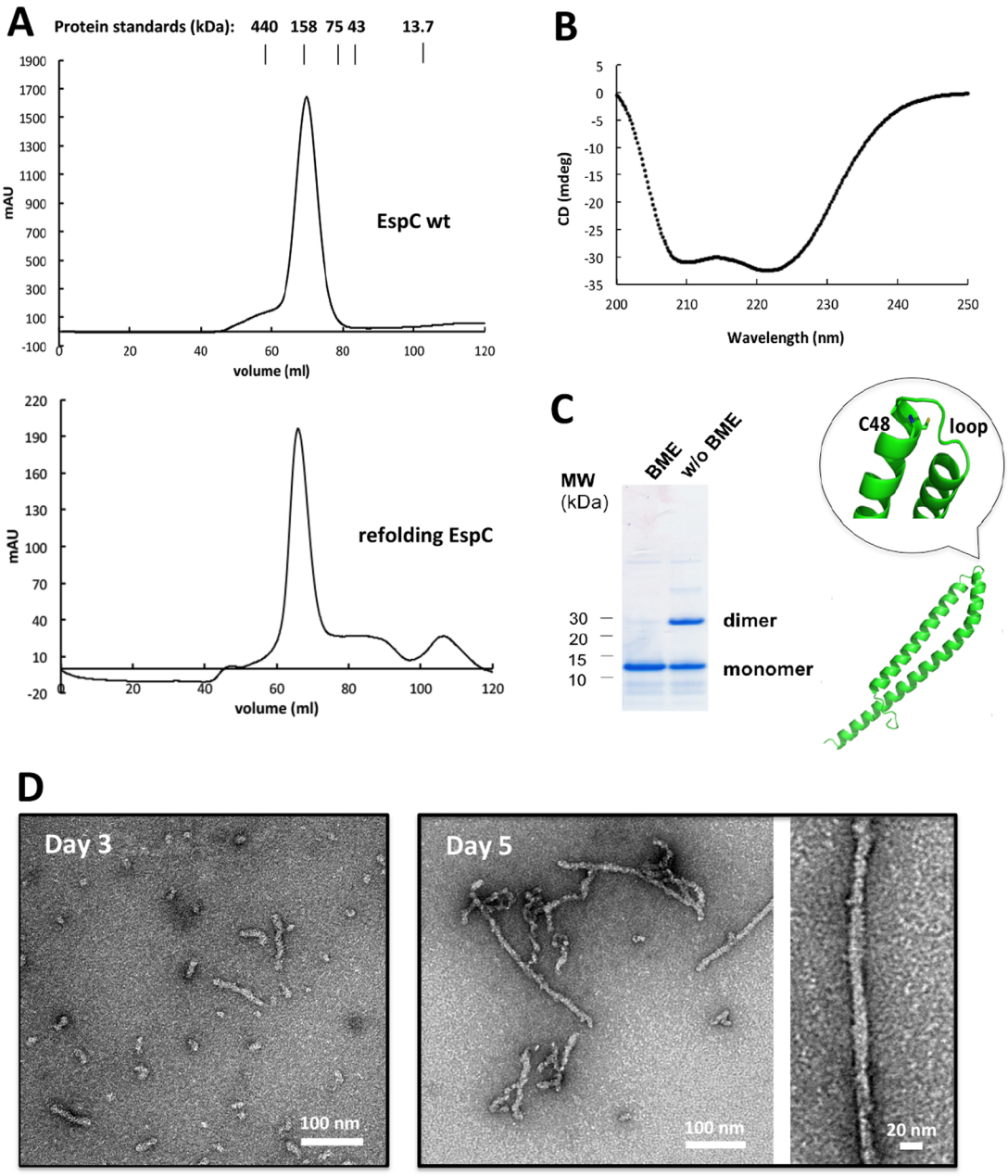

Fig. 4. Purified EspC self-polymerizes into a filamentous structure.
A. Size exclusion chromatography profile of recombinant EspC from *M. smegmatis* indicates its polymeric nature—top. Urea-denatured EspC refolds into a polymer similar to the natural state—bottom.
B. CD spectrum reveals polymer to be mainly α-helical.
C. Purified EspC was present as both dimer and monomer on an SDS-PAGE gel; the dimer became monomeric when treated with BME. In the predicted tertiary structure, Cys-48 localizes at the head of EspC.
D. Transmission electron micrographs of negatively stained filaments formed by recombinant EspC as a function of time. Filaments were variable in length and approximately 10–15 nm in diameter.

monomeric and multimeric forms (Fig. 5B), occurred in reduced amounts in the culture filtrate where less EsxA was present (Fig. 5D). *M. tb* expressing the EspC^{I98A} displayed an intermediate level of virulence (Fig. 5E). The other four residues mutated did not confer phenotypic differences compared with EspC^{wt} (Fig. 5F).

To establish whether the YxxxD signal motif is required for EspC secretion, site-directed mutagenesis was used to replace Tyr-87 and Asp-91 by alanine. EspC abundance was greatly affected by the Tyr87Ala substitution and the protein was only detected in the cell lysates. By contrast, although wild type levels of the

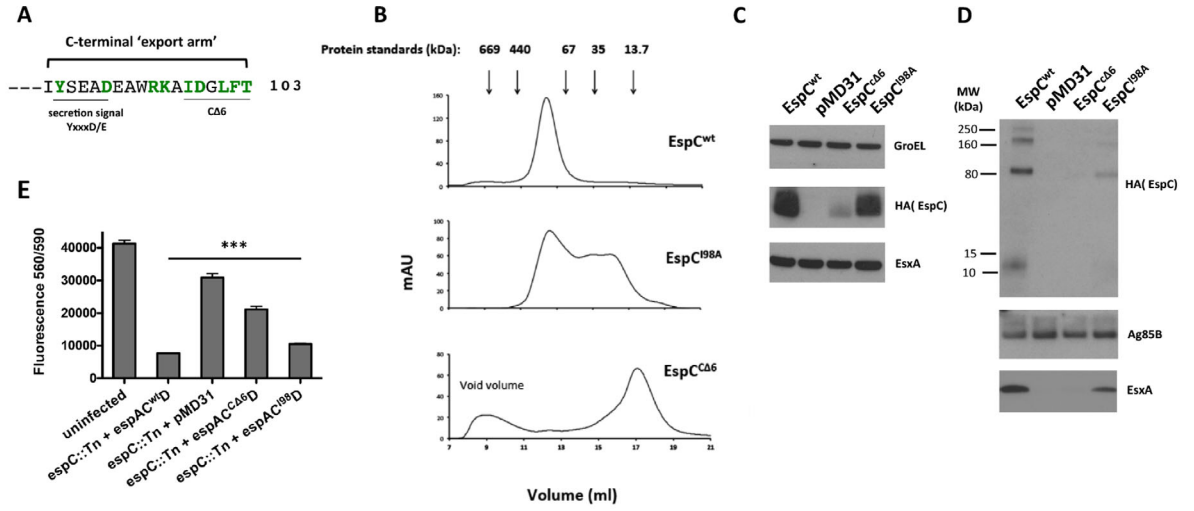

F

	EspC alleles												
	wt	C48S	D75A	Y87A	D91A	R95A	K96A	I98A	D99A	L101A	F102A	T103A	CΔ6
Stability	+	+/-	+	-	+	+	+	+/-	+	+	+	+	-
Exported	+	-	+	-	-	-	+	+/-	+	+	+	+	-
Multimers	+	+	+	NT	NT	+	+	+	+	+	+	+	-
EsxA Secreted	+	-	+	-	-	-	+	+/-	+	+	+	+	-
Attenuated	-	+/-	NT	+	+	+	NT	+/-	NT	-	NT	NT	+

Fig. 5. C-terminus of EspC is critical for stability, polymer assembly and ESX-1 function.
A. EspC harbours an 'export arm' at the C-terminus. The phenotypes of the indicated point mutations (in green) and a C-terminal tail truncated mutant (CΔ6) were investigated.
B. Compared with EspC^{wt} that was mainly polymeric on Superdex200 column chromatography, EspC^{CΔ6} was mainly monomeric, while the I98A variant behaved as a mixture of monomer and polymer, implying that the C-terminal region is critical for polymer assembly.
C. Loss of last 6 amino acids and the I98A mutation destabilized intracellular EspC, and D, impacted EsxA secretion.
E. Impact on ESX-1 function as indicated by reduced EsxA secretion and lower cytotoxicity compared with *M. tb* expressing wild type EspC. Mean + S.E.M. of triplicate measurements of a representative result from two independent experiments is depicted.
F. Summary of phenotypes of all EspC variants constructed in this study and their impact on protein stability, export, multimerization and cytotoxicity/attenuation. +, wild-type behaviour; −, no activity; ±, intermediate activity. NT, not tested.

Asp91Ala variant of EspC were found in the cells, none was detected in the culture filtrate. Both mutations also led to a complete block in EsxA secretion and cytotoxicity (Supporting Information Fig. S2).

Two point mutations between the YxxxD motif and the C-terminal tail, EspC^{R95A} and EspC^{K96A}, were also studied. EspC^{R95A} exhibited a striking phenotype, since it was only slightly less abundant in the cell lysate, but almost absent from the culture filtrate where EsxA was not detected. Similar to EspC^{CΔ6}, the R95A substitution caused severe attenuation of *M. tb* compared with the *espC*::Tn + *espAC^{wt}D* strain (Supporting Information Fig. S9).

These combined results indicate that the C-terminal 'export arm' region of EspC contributes to polymer formation, protein stability and export, as well as to the macrophage cytotoxicity of *M. tb*.

Discussion

It has long been known that the EspA/EspC proteins and the EsxA/EsxB heterodimer are mutually dependent for their secretion by the *M. tb* ESX-1 secretion system (Fortune *et al.*, 2005) but the underlying mechanism is unknown. A partial explanation for this codependency was provided by a recent investigation of the structure of the EccC multidomain ATPase in complex with EsxB (Rosenberg *et al.*, 2015). Binding of EsxB triggered multimerization and activation of EccC that then became functionally competent for type VII secretion. However, while this finding accounts for an early stage in the co-dependent secretion it does not explain the roles of EspA and EspC.

In our investigation, evidence for EspA-EspC interaction in the cytosol and the cell envelope was obtained

(Supporting Information Fig. S3). In the cytosol EspC appeared to be predominantly monomeric but was present in large SDS-resistant polymers in the cell membrane, capsular layer and culture filtrate of *M. tb*. Using either immunogold-EM or immunofluorescence microscopy to observe intact cells, we demonstrated that EspC was present in filaments exposed on the cell surface. Furthermore, on EM examination of cryo-sections of *M. tb* cells we observed similar filaments in and beyond the capsule of *M. tb*. In agreement with our EM images of *M. tb* cells and sections, recombinant EspC had a propensity to form filaments *in vitro* like those of the native protein. These filaments grew longer with time and exceeded 100 nm in length after a few days but were always about 10–15 nm in diameter.

Given that the EsxA/EsxB heterodimer depends on EspA/EspC for secretion and that EspC occurs outside the plasma membrane and in the capsule, we assessed the possible roles that EspC filaments might play in ESX-1 function by analogy with the more extensively characterized type II, III and IV secretion systems. The first possibility we considered was that EspC is a component of an outer membrane channel similar to that of the type IV secretion system of Gram negative bacteria. This channel is formed by a ring of VirB10 proteins, spanning the inner and outer membranes, which is lined with the VirB2 proteins that form the major pilin (Chandran *et al*., 2009). Depending on the bacterial species the VirB2 proteins contain from approximately 90 to 130 amino acid residues and are thus generally longer than EspC.

The second possibility is that EspC may function similarly to the major pseudopilin of type II secretion systems, formed by subunits such as XcpT, PulG or GspG from different bacterial species. Pseudopilin is assumed to function as a piston-like motor in the periplasm to push folded exoproteins across the outer membrane when the subunits polymerize (Douzi *et al*., 2012; Korotkov *et al*., 2012). Upon overexpression, long fibrillar structures, termed hyper-pseudopili that resemble type IV pili, can be observed (Durand *et al*., 2003; Vignon *et al*., 2003). However, EspC is smaller than the pseudopilin subunits that range in size from 140 to 160 residues.

The third possibility is that EspC could be analagous to the needle protein, the main component of the injectisome of the type III secretion system (T3SS) (Loquet *et al*., 2012). We note many common features, functionally and structurally, between EspC and the T3SS needle proteins, such as MxiH of *Shigella* and PrgI of *Salmonella*. The needle protein of the T3SS apparatus, at 83 residues, is smaller than EspC, composed of two α-helices linked by a loop, and is highly immunogenic. Purified T3SS needle proteins self-polymerize to form a helical filament in two-steps, nucleation then elongation (Poyraz *et al*., 2010; Loquet *et al*., 2012; Demers *et al*., 2013). Likewise, the α-helical EspC self-polymerizes, in a time-dependent manner and forms filaments that are far longer than those associated with bacterial cells (Fig. 4D).

The C-terminus is essential for MxiH or PrgI polymer formation upon secretion from the cytosol, as deletion of the last five amino acid residues causes defects in polymerization and needle formation (Kenjale *et al*., 2005; Poyraz *et al*., 2010). Purified EspC multimerizes *in vitro*, and this event is abolished by the C-terminal truncation, $EspC^{C\Delta6}$, implying that, in addition to the disulphide bond, the C-terminus mediates filament formation. Further proof of a critical role for the C-terminus is provided by the substitutions R95A and I98A that resulted in less EspC in the culture filtrate, less EsxA secretion and attenuation in *ex vivo* models (Fig. 5C–F; Supporting Information Fig. S9). These observations support the notion that the C-terminal 'export arm' of EspC (Solomonson *et al*., 2015) mediates polymer formation and bacterial virulence like its counterpart in the T3SS needle proteins. On the other hand, like the N-terminus of T3SS needle proteins, the N-terminus of EspC is plastic and can accommodate three different tags (His, HA and FLAG) without noticeably impacting its function.

Despite generating a large body of data, we are unable to distinguish between these three possibilities, or others such as an indirect role, and further research is required to establish the precise composition and structure of the EspC-containing filaments that may represent an ESX-1 secretion channel. This will also enable us to establish what other proteins are present in these filamentous structures and to clarify the role of EspF in *M. tb*.

Experimental procedures

Bacterial strains and culture conditions

M. tb and *M. smegmatis* were routinely grown in 7H9 broth supplemented with 0.2% glycerol, 10% ADC, 0.05% Tween-80 or on 7H11 agar supplemented with 0.5% glycerol and 10% OADC. The *M. smegmatis groEL1ΔC* strain used for EspC production was cultured in 7H9 broth containing 0.2% glycerol, 0.05% Tween-80, 0.2% glucose and 50 μg ml^{-1} hygromycin. *M. tb espC*::Tn + *espACD* and *espC*::Tn + pMD31 were grown in medium containing 25 μg ml^{-1} kanamycin and 50 μg ml^{-1} hygromycin. *E. coli* TOP 10 (Invitrogen) used for cloning and propagation was grown on Luria–Bertani agar or broth.

Overexpression, purification and oligomeric state analysis

M. tb EspC was PCR amplified and cloned into the vector pMyNT and used to generate EspC mutant constructs by site-directed mutagenesis with Pfu polymerase (Promega).

These plasmids were transformed into *M. smegmatis groEL1ΔC* strain (EMBL, Hamburg) by electroporation. EspC overexpression was induced with acetamide when the bacteria were grown to OD_{600} 0.6–0.8. After 30 h at 25˚C, the cells were harvested and resuspended in lysis buffer containing 20 mM Tris pH8.0, 500 mM NaCl, 1 M urea, 0.5% Triton X-100, 5% glycerol, 10 mM imidazole and 2 mM BME with protease inhibitor cocktail and DNase I (Roche). Cells were lysed with an EmulsiFlex-C3 homogenizer followed by centrifugation to remove insoluble debris. N-terminally His-tagged EspC present in the supernatant was subjected to nickel affinity purification (Ni-NTA agarose, Invitrogen) and eluted with 20 mM Tris pH 8.0, 500 mM NaCl, 300 mM imidazole, 2 mM BME. Size exclusion chromatography (Hiload 16/60 Superdex200 column, GE Healthcare) was used to further purify the recombinant EspC with elution buffer containing 20 mM Tris pH8.0, 500 mM NaCl and 2 mM BME. Fractions were analyzed by SDS-PAGE.

The same lysis buffer but containing 8 M urea was used to denature proteins in the cell lysate that were then loaded onto a nickel affinity column. After dialyzing the eluate to remove urea, size exclusion chromatography was performed on a Superdex200 (16/60) column to analyze the refolded proteins. To establish the oligomeric state of EspC and its mutants, the purified proteins were loaded onto a Superdex200 (10/300GL) column (GE Healthcare) and eluted with buffer containing 20 mM Tris pH 8.0, 500 mM NaCl and 2 mM BME. Molecular weights of the proteins were estimated according to protein standards.

Circular dichroism (CD) measurement

EspC was diluted to 0.375 mg ml^{-1}, transferred into a quartz cuvette of 1 mm path length and analyzed using a Jasco J-815 CD spectrometer. Due to strong UV absorbance of chloride ions at low wavelengths, the far-UV CD spectra were recorded between 200 and 250 nm. Spectra were acquired in triplicate and averaged after subtracting the buffer background.

Filament formation in vitro and transmission electron microscopy (TEM)

Purified EspC (in 20 mM Tris pH8.0, 500 mM NaCl) was diluted to 1.8 mg ml^{-1} (20 mM Tris pH8.0, 50 mM NaCl) and analyzed after 3 days and 5 days at room temperature without shaking. After a short centrifugation at 10k rpm, the supernatant was applied to glow-discharged, carbon-coated 400 mesh grid (Canemco-Marivac) and stained with 2% uranyl acetate. Samples were viewed using TEM (Tecnai Spirit BioTWIN).

Macrophage cytotoxicity assay

Macrophage viability was evaluated using potassium efflux measurement. Cell monolayers (mouse macrophage-like cell line RAW 264.7) were washed with PBS, and 1 ml of DMEM (buffered with HEPES pH 7.4 and 1 μg ml^{-1} of trypsin/chymotrypsin inhibitor) was added to the wells. Cells were incubated with 100 μg ml^{-1} and 50 μg ml^{-1} of purified EspC for 2 h followed by washing once with choline buffer (139 mM cholineCl, 0.8 mM $MgCl_2$, 1.5 mM $CaCl_2$, 5 mM citric acid, 5.6 mM glucose, 10 mM NH_4Cl and 5 mM H_3PO_4, pH7.4). EsxA (30 μg ml^{-1}) and EccA1 (1-280; 100 μg ml^{-1}) were used as positive and negative controls respectively. After incubating in lysis buffer (choline buffer with 0.5% TritonX-100) for 30 min, the potassium content in the cell lysate was determined using a Sherwood M410 Flame photometer.

Genetic complementation of EspC transposon insertion mutant

Plasmid pMD31-*espACD* contains the *espACD* operon preceded by 568 bp of DNA upstream of the *espA* start codon (Chen *et al.*, 2012). The Erdman *espC*::Tn (Hyg^r) mutant was described previously (Dhar and McKinney, 2010). The sequence encoding the HA epitope was inserted into the 5′-end of *espC* by Quick Change Mutagenesis (KAPA HiFi HotStart PCR kits, KAPA Biosystems). This plasmid and the pMD31 empty vector were transformed into the *espC*::Tn mutant strain by electroporation. Transformants were selected on 7H11 agar plates containing 25 μg ml^{-1} kanamycin and 50 μg ml^{-1} hygromycin.

Preparation of culture filtrates, cell lysates and capsule extracts

To analyze protein production and secretion, *M. tb espC*::Tn + $espAC_{HA}D$ and *espC*::Tn + pMD31 strains were grown in Sauton's medium (plus 0.002% Tween-80) with a starting OD_{600} 0.1. After 6 days growth at 37˚C, culture filtrates and cell lysates, were prepared as described (Chen *et al.*, 2012). Cell membrane was separated from the crude lysate by ultracentrifugation at 125 000*g* for 1 h. Capsule layer proteins were extracted using 0.25% Genapol X-080 and enriched by TCA-precipitation (Sani *et al.*, 2010). Total protein concentration was determined using the BCA assay (Thermo Scientific).

Protein analysis by immunoblotting

Culture filtrates, cell lysates and capsule extracts were analyzed by SDS-PAGE and immunoblotting as previously described (Chen *et al.*, 2012). For EspC, equivalent amounts of total proteins were boiled in SDS sample buffer with and without 5 mM DTT before gel electrophoresis. HA-tagged EspC was detected with HRP-conjugated anti-HA mouse monoclonal antibody (Cell Signaling, #2999). Anti-EsxA (Abcam, ab26246) and anti-GroEL (Abcam, ab20045) mouse monoclonal antibodies, recognized by peroxidase (HRP) conjugated anti-mouse IgG antibodies (Sigma-Aldrich), were used respectively for EsxA and GroEL detection. Anti-Ag85 (Abcam, ab43019) and Anti-CFP10 (Abcam, ab45074) rabbit polyclonal antibodies, recognized by HRP conjugated anti-rabbit antibodies (Sigma-Aldrich).

Macrophage infection assay

Phorbol myristate (50 nM) activated THP-1 cells (2×10^6 ml^{-1}) were seeded in complete RPMI medium in a 96-well plate, infected with *M. tb* strains at a multiplicity of infection of 5 and incubated for 48 h at 37˚C under 5% CO_2. Cytotoxicity was evaluated by measuring cell viability using PrestoBlue Cell Viability Reagent (Invitrogen).

Co-immunoprecipitation

Total cell lysate proteins (1 mg) of *M. tb* strains *espC*::Tn + *espAC*$_{HA}$*D* and *espC*::Tn + *espACD* were added to 20 μl of agarose-conjugated anti-HA monoclonal antibody (Sigma-Aldrich) and incubated at 4˚C for 4 h. Beads were washed five times with PBS, eluted with 80 μl SDS sample buffer and boiled for 3 min prior to electrophoresis. Eluted proteins were analyzed by silver staining (SilverQuest™ Silver Stain Kit, Invitrogen) or by LC-MS/MS and immunoblotting.

LC-MS/MS analysis

Bands of interest were excised from SDS-PAGE gels and In-Gel digested using modified trypsin. Extracted peptides were then concentrated using a vacuum concentrator and analyzed by LC-MS/MS. Samples were separated by Reverse Phase on a Dionex RSLC Ultimate 3000nano UPLC connected in-line with an Orbitrap Elite high resolution Mass Spectrometer (Thermo Fisher Scientific). Chromatographic separation was performed over a 80 min gradient using a capillary column (Nikkyo Technos Co; C18; 3 μm-100 Å; 15 cm × 75 μm ID) at 250 nl min^{-1}. Data dependent acquisition mode was used with dynamic exclusion where the first 20 parent ions were fragmented and then excluded for the following 30 seconds. Database searching was performed with Proteome Discoverer 1.4 using Mascot 2.3 and Sequest HT as search engines against the TubercuList R27 FASTA Database. Met oxidation, Ser-Thr-Tyr phosphorylation and peptide N-acetylation were set as variable modifications while Cys carbamidomethylation was set as fixed modification. Final data inspection was carried out with Scaffold.

Immunogold-EM and immunofluorescence-microscopy

For immuno-labelling of whole cell mounts, *M. tb* *espC*::Tn + *espAC*$_{HA}$*D* and *espC*::Tn + pMD31 were cultured in Sauton's medium (without Tween) for 3 days to exponential growth phase when 5 ml of culture were mixed with equal volume of PBS buffer containing 4% paraformaldehyde and 0.4% glutaraldehyde and fixed for 90 min. Cells were pelleted and resuspended in 200 μl PBS containing 0.15 M glycine. Samples were incubated on formvar coated 200 mesh grids (Canemco-Marivac) for 10 min, then blocked with 1% BSA in PBS for 10 min prior to incubating with anti-HA mouse monoclonal antibody (Cell Signaling, #2367, 1/40 dilution) for 75 min. After washing twice with PBS and twice with 1% BSA-PBS, grids were incubated in PBS containing 1% BSA and anti-Mouse IgG (1/50 dilution) conjugated with 10 nm gold particles (Electron Microscopy Science, #25129) for 2 h. Grids were then washed four times with PBS and air dried before observation by TEM. For sectioning, cells were chemically fixed with a buffered mix of 2% paraformaldehyde and 0.1% glutaraldehyde, and embedded in 12% gelatin. Small cubes (1 mm width) were then infiltrated overnight in 20% sucrose before freezing in liquid nitrogen. These were then sectioned at −100˚C to a thickness of 100 nm using an ultramicrotome (Leica UC7/FCS, Leica Microsystems, Vienna). Sections were collected on grids carrying a drop of methyl-cellulose at room temperature. These were then processed for immunogold labelling as above.

For immunofluorescent staining, fixed bacterial suspensions were loaded onto coverslips pretreated with 0.01% poly-L-lysine, blocked with 1% BSA-PBS for 30 min and incubated with anti-HA antibody (1/100 dilution) for 90 min. Subsequently, the cells were stained with Alexa Fluor-488 anti-mouse antibody (Life Technologies, 1/200 dilution) for 1 h and analyzed using a fluorescence microscope (ZeissAxio Imager Z1). The same exposure was used for *espC*::Tn + *espAC*$_{HA}$*D* and *espC*::Tn + pMD31 when imaging fluorescence.

Acknowledgements

We thank Stefanie Boy and Philippe Busso for technical assistance; Jeffery Chen, Florence Pojer, and Nicole van der Wel for advice and encouragement; Graham Knott and Stephanie Clerc-Rosset (EPFL Bioelectron Microscopy Core Facility) for help with EM and Diego Chiappe (EPFL Proteomics Core Facility) for performing LC-MS/MS. This project was funded by the Swiss National Science Foundation under grants n°31003A-140778 and n°31003A-162641.

Author contributions

Conceived and designed the experiments: YL JR CS and STC. Performed the experiments: YL. Analyzed the data: all authors. Wrote the article: YL JR STC.

Conflict of interest statement

The authors declare no conflict of interest.

References

Bitter, W., Houben, E.N., Bottai, D., Brodin, P., Brown, E.J., Cox, J.S., et al. (2009) Systematic genetic nomenclature for type VII secretion systems. *PLoS Pathog* **5**: e1000507.

Brennan, P.J., and Nikaido, H. (1995) The envelope of mycobacteria. *Annu Rev Biochem* **64**: 29–63.

Brodin, P., Majlessi, L., Marsollier, L., De Jonge, M.I., Bottai, D., Demangel, C., *et al.* (2006) Dissection of ESAT-6 system 1 of Mycobacterium tuberculosis and

impact on immunogenicity and virulence. *Infect Immun* **74**: 88–98.
Champion, P.A., Stanley, S.A., Champion, M.M., Brown, E.J., and Cox, J.S. (2006) C-terminal signal sequence promotes virulence factor secretion in Mycobacterium tuberculosis. *Science* **313**: 1632–1636.
Champion, P.A., Champion, M.M., Manzanillo, P., and Cox, J.S. (2009) ESX-1 secreted virulence factors are recognized by multiple cytosolic AAA ATPases in pathogenic mycobacteria. *Mol Microbiol* **73**: 950–962.
Chandran, V., Fronzes, R., Duquerroy, S., Cronin, N., Navaza, J., and Waksman, G. (2009) Structure of the outer membrane complex of a type IV secretion system. *Nature* **462**: 1011–1015.
Chen, J.M., Boy-Rottger, S., Dhar, N., Sweeney, N., Buxton, R.S., Pojer, F., *et al*. (2012) EspD is critical for the virulence-mediating ESX-1 secretion system in Mycobacterium tuberculosis. *J Bacteriol* **194**: 884–893.
Cole, S.T., Eiglmeier, K., Parkhill, J., James, K.D., Thomson, N.R., Wheeler, P.R., *et al*. (2001) Massive gene decay in the leprosy bacillus. *Nature* **409**: 1007–1011.
Daleke, M.H., Ummels, R., Bawono, P., Heringa, J., Vandenbroucke-Grauls, C.M., Luirink, J., *et al*. (2012) General secretion signal for the mycobacterial type VII secretion pathway. *Proc Natl Acad Sci U S A* **109**: 11342–11347.
Das, C., Ghosh, T.S., and Mande, S.S. (2011) Computational analysis of the ESX-1 region of Mycobacterium tuberculosis: insights into the mechanism of type VII secretion system. *PLoS One* **6**: e27980.
Daugelat, S., Kowall, J., Mattow, J., Bumann, D., Winter, R., Hurwitz, R., and Kaufmann, S.H. (2003) The RD1 proteins of Mycobacterium tuberculosis: expression in Mycobacterium smegmatis and biochemical characterization. *Microbes Infect* **5**: 1082–1095.
De Jonge, M.I., Pehau-Arnaudet, G., Fretz, M.M., Romain, F., Bottai, D., Brodin, P., *et al*. (2007) ESAT-6 from Mycobacterium tuberculosis dissociates from its putative chaperone CFP-10 under acidic conditions and exhibits membrane-lysing activity. *J Bacteriol* **189**: 6028–6034.
De Leon, J., Jiang, G., Ma, Y., Rubin, E., Fortune, S., and Sun, J. (2012) Mycobacterium tuberculosis ESAT-6 exhibits a unique membrane-interacting activity that is not found in its ortholog from non-pathogenic Mycobacterium smegmatis. *J Biol Chem* **287**: 44184–44191.
Demers, J.P., Sgourakis, N.G., Gupta, R., Loquet, A., Giller, K., Riedel, D., *et al*. (2013) The common structural architecture of Shigella flexneri and Salmonella typhimurium type three secretion needles. *PLoS Pathog* **9**: e1003245.
Dhar, N., and McKinney, J.D. (2010) Mycobacterium tuberculosis persistence mutants identified by screening in isoniazid-treated mice. *Proc Natl Acad Sci U S A* **107**: 12275–12280.
Douzi, B., Filloux, A., and Voulhoux, R. (2012) On the path to uncover the bacterial type II secretion system. *Philos Trans R Soc Lond B Biol Sci* **367**: 1059–1072.
Durand, E., Bernadac, A., Ball, G., Lazdunski, A., Sturgis, J.N., and Filloux, A. (2003) Type II protein secretion in Pseudomonas aeruginosa: the pseudopilus is a multifibrillar and adhesive structure. *J Bacteriol* **185**: 2749–2758.
Fortune, S.M., Jaeger, A., Sarracino, D.A., Chase, M.R., Sassetti, C.M., Sherman, D.R., *et al*. (2005) Mutually dependent secretion of proteins required for mycobacterial virulence. *Proc Natl Acad Sci U S A* **102**: 10676–10681.
Guinn, K.M., Hickey, M.J., Mathur, S.K., Zakel, K.L., Grotzke, J.E., Lewinsohn, D.M., *et al*. (2004) Individual RD1-region genes are required for export of ESAT-6/CFP-10 and for virulence of Mycobacterium tuberculosis. *Mol Microbiol* **51**: 359–370.
Houben, E.N., Bestebroer, J., Ummels, R., Wilson, L., Piersma, S.R., Jimenez, C.R., *et al*. (2012) Composition of the type VII secretion system membrane complex. *Mol Microbiol* **86**: 472–484.
Hsu, T., Hingley-Wilson, S.M., Chen, B., Chen, M., Dai, A.Z., Morin, P.M., *et al*. (2003) The primary mechanism of attenuation of bacillus Calmette-Guerin is a loss of secreted lytic function required for invasion of lung interstitial tissue. *Proc Natl Acad Sci U S A* **100**: 12420–12425.
Kenjale, R., Wilson, J., Zenk, S.F., Saurya, S., Picking, W.L., Picking, W.D., and Blocker, A. (2005) The needle component of the type III secreton of Shigella regulates the activity of the secretion apparatus. *J Biol Chem* **280**: 42929–42937.
Korotkov, K.V., Sandkvist, M., and Hol, W.G. (2012) The type II secretion system: biogenesis, molecular architecture and mechanism. *Nat Rev Microbiol* **10**: 336–351.
Loquet, A., Sgourakis, N.G., Gupta, R., Giller, K., Riedel, D., Goosmann, C., Griesinger, C., *et al*. (2012) Atomic model of the type III secretion system needle. *Nature* **486**: 276–279.
Mah, N., Perez-Iratxeta, C., and Andrade-Navarro, M.A. (2010) Outer membrane pore protein prediction in mycobacteria using genomic comparison. *Microbiology* **156**: 2506–2515.
Millington, K.A., Fortune, S.M., Low, J., Garces, A., Hingley-Wilson, S.M., Wickremasinghe, M., *et al*. (2011) Rv3615c is a highly immunodominant RD1 (Region of Difference 1)-dependent secreted antigen specific for Mycobacterium tuberculosis infection. *Proc Natl Acad Sci U S A* **108**: 5730–5735.
Niederweis, M., Danilchanka, O., Huff, J., Hoffmann, C., and Engelhardt, H. (2010) Mycobacterial outer membranes: in search of proteins. *Trends Microbiol* **18**: 109–116.
Noens, E.E., Williams, C., Anandhakrishnan, M., Poulsen, C., Ehebauer, M.T., and Wilmanns, M. (2011) Improved mycobacterial protein production using a Mycobacterium smegmatis groEL1DeltaC expression strain. *BMC Biotechnol* **11**: 27.
Poyraz, O., Schmidt, H., Seidel, K., Delissen, F., Ader, C., Tenenboim, H., *et al*. (2010) Protein refolding is required for assembly of the type three secretion needle. *Nat Struct Mol Biol* **17**: 788–792.
Pym, A.S., Brodin, P., Brosch, R., Huerre, M., and Cole, S.T. (2002) Loss of RD1 contributed to the attenuation of the live tuberculosis vaccines Mycobacterium bovis BCG and Mycobacterium microti. *Mol Microbiol* **46**: 709–717.
Renshaw, P.S., Panagiotidou, P., Whelan, A., Gordon, S.V., Hewinson, R.G., Williamson, R.A., and Carr, M.D. (2002) Conclusive evidence that the major T-cell antigens of the Mycobacterium tuberculosis complex ESAT-6 and CFP-

10 form a tight, 1:1 complex and characterization of the structural properties of ESAT-6, CFP-10, and the ESAT-6*CFP-10 complex. Implications for pathogenesis and virulence. *J Biol Chem* **277**: 21598–21603.

Rosenberg, O.S., Dovala, D., Li, X., Connolly, L., Bendebury, A., Finer-Moore, J., *et al.* (2015) Substrates control multimerization and activation of the multi-domain atpase motor of type vii secretion. *Cell* **161**: 501–512.

Sani, M., Houben, E.N., Geurtsen, J., Pierson, J., de Punder, K., van Zon, M., *et al.* (2010) Direct visualization by cryo-EM of the mycobacterial capsular layer: a labile structure containing ESX-1-secreted proteins. *PLoS Pathog* **6**: e1000794.

Simeone, R., Bottai, D., and Brosch, R. (2009) ESX/type VII secretion systems and their role in host-pathogen interaction. *Curr Opin Microbiol* **12**: 4–10.

Smith, J., Manoranjan, J., Pan, M., Bohsali, A., Xu, J., Liu, J., *et al.* (2008) Evidence for pore formation in host cell membranes by ESX-1-secreted ESAT-6 and its role in Mycobacterium marinum escape from the vacuole. *Infect Immun* **76**: 5478–5487.

Solomonson, M., Setiaputra, D., Makepeace, K.A., Lameignere, E., Petrotchenko, E.V., Conrady, D.G., *et al.* (2015) Structure of EspB from the ESX-1 type VII secretion system and insights into its export mechanism. *Structure* **23**: 571–583.

Stanley, S.A., Raghavan, S., Hwang, W.W., and Cox, J.S. (2003) Acute infection and macrophage subversion by Mycobacterium tuberculosis require a specialized secretion system. *Proc Natl Acad Sci U S A* **100**: 13001–13006.

Stoop, E.J., Bitter, W., and van der Sar, A.M. (2012) Tubercle bacilli rely on a type VII army for pathogenicity. *Trends Microbiol* **20**: 477–484.

Sysoeva, T.A., Zepeda-Rivera, M.A., Huppert, L.A., and Burton, B.M. (2014) Dimer recognition and secretion by the ESX secretion system in Bacillus subtilis. *Proc Natl Acad Sci U S A* **111**: 7653–7658.

Van der Woude, A.D., Mahendran, K.R., Ummels, R., Piersma, S.R., Pham, T.V., Jimenez, C.R., *et al.* (2013) Differential detergent extraction of mycobacterium marinum cell envelope proteins identifies an extensively modified threonine-rich outer membrane protein with channel activity. *J Bacteriol* **195**: 2050–2059.

Vandal, O.H., Nathan, C.F., and Ehrt, S. (2009) Acid resistance in Mycobacterium tuberculosis. *J Bacteriol* **191**: 4714–4721.

Vignon, G., Kohler, R., Larquet, E., Giroux, S., Prevost, M.C., Roux, P., and Pugsley, A.P. (2003) Type IV-like pili formed by the type II secreton: specificity, composition, bundling, polar localization, and surface presentation of peptides. *J Bacteriol* **185**: 3416–3428.

Wards, B.J., de Lisle, G.W., and Collins, D.M. (2000) An esat6 knockout mutant of Mycobacterium bovis produced by homologous recombination will contribute to the development of a live tuberculosis vaccine. *Tuber Lung Dis* **80**: 185–189.

Zumla, A., George, A., Sharma, V., Herbert, R.H., Oxley, A., and Oliver, M. (2015) The WHO 2014 global tuberculosis report–further to go. *Lancet Glob Health* **3**: e10–e12.

Supporting information

Additional supporting information may be found in the online version of this article at the publisher's web-site.